Neutron Larmor Diffraction study of the $BaM_2(XO_4)_2$ (M = Co, Ni; X = As, P) compounds

Journal of Physics: Conference Series **340** (2012) 012012 doi:10.1088/1742-6596/340/1/012012

Neutron Larmor Diffraction study of the $BaM_2(XO_4)_2$ (M = Co, Ni; X = As, P) compounds

Nicolas Martin[1], Louis-Pierre Regnault[1] and Serguei Klimko[2]

[1] SPSMS, UMR-E CEA / UJF-Grenoble 1, INAC, Grenoble, F-38054, France
[2] Laboratoire Léon Brillouin, CEA-CNRS, CEA/Saclay, 91191 Gif sur Yvette, France

E-mail: regnault@ill.fr

Abstract. Neutron Larmor Diffraction is a relatively new concept in neutron scattering which allows high resolution studies of subtle structural features in condensed matter. Several setups exist in various neutron facilities around the world. One of them is the Zero-field spin-Echo for Triple-Axis option (ZETA), available on the thermal triple-axis spectrometer IN22 (CEA-CRG beamline at Institut Laue Langevin). We have used ZETA to study thermal evolution of lattice constants in serveral systems of physical interest. Among them, the $BaM_2(XO_4)_2$ family is a serie of compounds which have been intensively studied for three decades, mainly because of their fundamental though puzzling magnetic properties. In this paper, we aim to shed a new light on the physical understanding of those systems by investigating the link between structural and magnetic ordering. The magnetoelastic effect is found to be weak but can be resolved thanks to the high resolution provided by NLD.

1. Introduction

Materials with strong magnetoelastic couplings are the subject of a large number of studies because of their certain proximity to a multiferroic state. For instance, this point has been stressed in the case of hexagonal manganites $RMnO_3$ ([1]). However, magnetostriction is a more general property of magnetic materials and is observed in many systems. To probe the existence of such a coupling between spin and lattice degrees of freedom in the $BaM_2(XO_4)_2$ family, we chose to measure the thermal evolution of lattice constants in three systems belonging to this serie by using Neutron Larmor Diffraction (NLD). Interestingly, all of them cristallize within the same space group but display different magnetic structures when cooled below their respective Néel temperature. In the following, we will introduce the main features and interesting facts about the studied compounds (Sec. 2). As already reported elsewhere (*e.g.* in [2]), a state of the art Zero-field spin-Echo for Triple-Axis (ZETA) option has been recently commisionned and is now available on the thermal TAS spectrometer IN22. Initially designed for studying lifetimes of elementary excitations in different class of single-crystalline samples, this setup can easily be operated into a high resolution diffraction mode using NLD. This elegant method allows to circumvent the usual tight compromise between intensity and resolution. A handwaving explanation of its principle and the specificities of the ZETA option will be given (Sec. 3). Finally, we will present the results obtained on the thermal lattice response of $BaM_2(XO_4)_2$ (Sec. 4).

2. Basic properties of the $BaM_2(XO_4)_2$-family

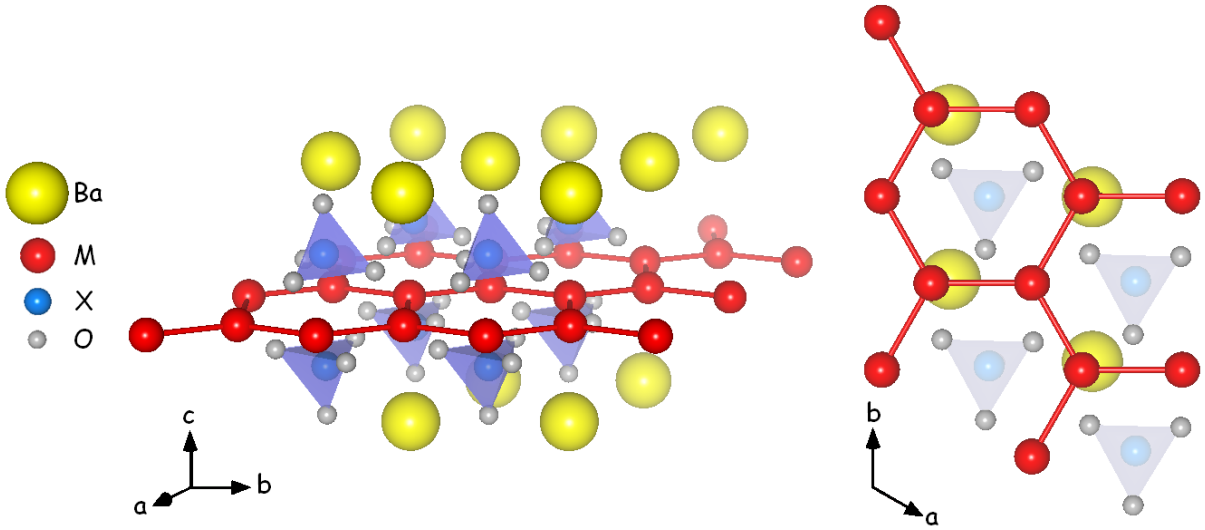

Figure 1. General structure of $BaM_2(XO_4)_2$ compounds. Each plane is monoatomic. Magnetic ions (in red) form a honeycomb lattice.

Table 1. Basic properties of the $BaM_2(XO_4)_2$ compounds studied in this paper. Lattice parameters are given at T = 4.2 K and d_2/d_1 is the ratio between the in-plane and interplane M-M distances.

Formula	a (Å)	c (Å)	d_2/d_1
$BaNi_2(PO_4)_2$	4.81	23.22	2.78
$BaNi_2(AsO_4)_2$	4.94	23.43	2.85
$BaCo_2(AsO_4)_2$	5.00	23.25	2.89

$BaM_2(XO_4)_2$, with M being a transition metal (Co or Ni) and X a pnictogen (As or P) is a family of compounds with interesting magnetic properties. All of them crystallize within the rhombohedral space group $R\bar{3}$ and no strucural phase transition has ever been measured down to the lowest temperature. Their layered structure consists in a stacking of atomic planes where magnetic ions sit on a honeycomb lattice. Theses planes are well separated from each other which naturally makes $BaM_2(XO_4)_2$ a very good playground to study two-dimensionnal magnetism (see Fig. 1 and Tab. 1). For instance, this 2-d character is evidenced by inelastic neutron scattering and the presence of a T^2-term in the low temperature specific heat ([3]). On the other hand, magnetization and neutron diffraction measurements reveal a strong planar spin anisotropy. From the microscopic magnetism point of view, each compound behave differently upon cooling. All of them order at finite temperatures but, even if their nuclear structure stays the same, different structures, *i.e.* described by different $\vec{k}$-vectors, arise. In Tab.2, we give the different exchange integrals determined from the analaysis of spin waves dispersion laws. We note that in each case, the third neighbour exchange integral is negative. In $BaNi_2(PO_4)_2$, $\mathcal{J}_1$ and $\mathcal{J}_2$ are also negative but in arsenides, they are positive. In fact, it is helpful to define an

effective exchange integral for each compound like $\tilde{\mathcal{J}} = -E(\vec{k})/3\mathcal{S}^2$, where $E(\vec{k})$ is the classical energy of the ground state. $\tilde{\mathcal{J}}$ is actually a measure of the interactions present in these systems. Measurement of the thermal evolution of the magnetic moment yields different behaviours for each sample. If we define a critical scaled temperature like $t_c = T_N/|\tilde{\mathcal{J}}|\mathcal{S}(\mathcal{S}+1)$, it follows that the lower t_c is, the steeper the moment variation will be (see Fig. 2). Those differences motivated us to lead a comparative study of their thermal expansion properties along both in-plane and out-of-plane axis to probe the existence of a hypothetical magnetoelastic coupling and the differences which may appear.

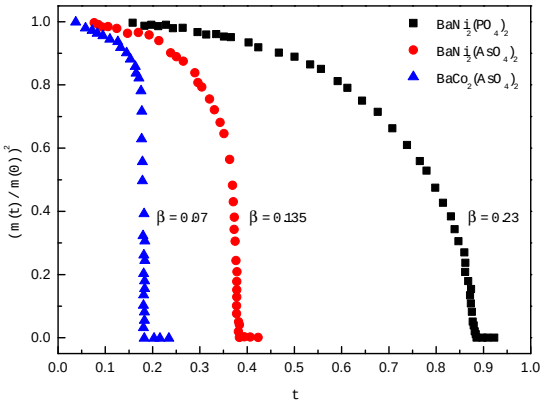

Figure 2. Square of the magnetic moment obtained by neutron diffraction plotted as a function of the reduced temperature $t = T/|\tilde{\mathcal{J}}|\mathcal{S}(\mathcal{S}+1)$. Fitting the data to a power law of the form $I(T)/I(0) = A(1 - T/T_N)^{2\beta}$ yields dramatically different critical exponents β.

Table 2. Magnetic properties of the $BaM_2(XO_4)_2$ compounds studied in this paper. $\mathcal{S}$ is the spin born by magnetic ions, $\mathcal{J}_1$, $\mathcal{J}_2$ and $\mathcal{J}_3$ are respectively the first, second and third nearest neighbour exchange integrals, T_N is the Neel temperature, β the critical exponent and $\vec{k}$ is the propagation vector of the magnetic structure in each compound (from [4]).

Formula	$\mathcal{S}$	$\mathcal{J}_1/k_b$ (K)	$\mathcal{J}_2/k_b$ (K)	$\mathcal{J}_3/k_b$ (K)	T_N (K)	β	$\vec{k}$
$BaNi_2(PO_4)_2$	1	-2.2	-0.3	-8.8	24	0.23	(0, 0, 0)
$BaNi_2(AsO_4)_2$	1	3.4	0.2	-10.0	18.5	0.135	(0.5, 0, 0.5)
$BaCo_2(AsO_4)_2$	1/2	38	1.5	-10.0	5.35	0.07	(0.27, 0, -1.33)

3. Neutron Larmor Diffraction with ZETA

Neutron Larmor Diffraction (NLD) is now well established as a powerful derivative of Neutron Spin Echo for structural studies in condensed matter physics. To understand how this technique works, let us first consider a general feature of elastic neutron scattering. Bragg condition selects the component of the neutron wavevector perpendicular to the lattice planes involved in the very process of diffraction according to the following vector relation:

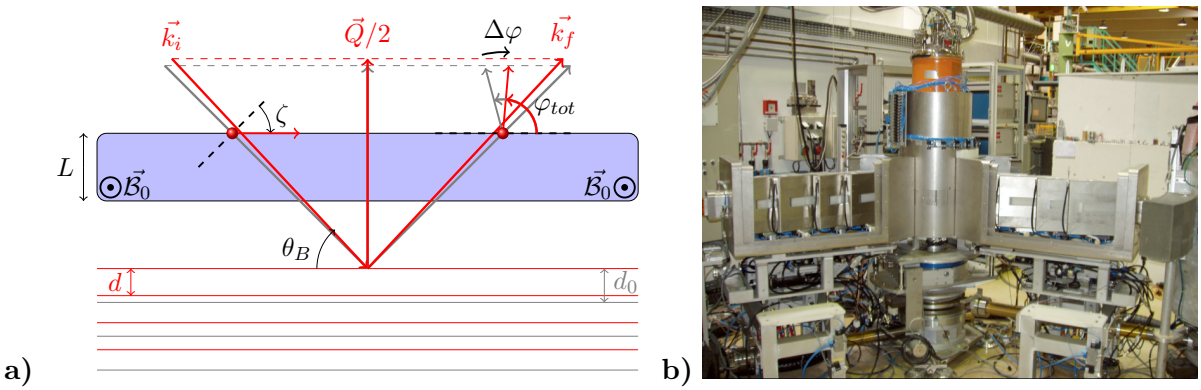

Figure 3. *a)* Layout depicting the principle of NLD. *b)* ZETA option as installed on IN22. The upper part of the μ-metal shielding is removed to show the four pairs of radio-frequency spin flippers (see text).

$$\vec{k}\sin\theta_B = \vec{Q}/2 \tag{1}$$

where $|\vec{k}| = m_n v/\hbar$ and $|\vec{Q}| = 2\pi/d$ with m_n the neutron mass, v its velocity and d the lattice spacing being measured. The latter equation means that the scattering angle is completely controlled by d (or its reciprocal space counterpart, $|\vec{Q}|$) for a given neutron velocity v (or wavevector $|\vec{k}|$). In general, a neutron beam contains a distribution of $\vec{k}$ and the evaluation of d is consequently vitiated by an error calculated as follows:

$$\frac{\delta d}{d} = \left(\left(\frac{\delta k}{k}\right)^2 + \left(\frac{\delta\theta_B}{\theta_B}\right)^2 \cot^2\theta_B\right)^{1/2} \tag{2}$$

Thus, measuring d with high accuracy can be done by conventionnal neutron diffraction (CND) but this requires a tight collimation of the beam. This naturally results in a loss of intensity as while constraining neutrons trajectories, the ones which can travel through the apparatus become more and more scarce. To circumvent this limitation, it has been proposed to measure neutrons velocity, and hence d, by means of Larmor precession using a setup such as the one which is sketched in Fig. 3 *a)* ([5]). The neutron beam is first polarized. After passing through the apparatus, the total phase, *i.e.* the rotation angle of the neutron magnetic moment around the magnetic field $\vec{\mathcal{B}}_0$, is simply proportional to the time spent by each neutron within this field region and hence to sample dependent quantities:

$$\varphi_{tot}(d) = \omega_L t = \frac{\omega_L L}{v\cos\zeta} = 4\frac{m_n\omega_L L}{h}\cdot\frac{\sin\theta_B}{\cos\zeta}\cdot d \tag{3}$$

where $\omega_L = \gamma_n|\vec{\mathcal{B}}_0|$ is the Larmor pulsation associated with the field $\vec{\mathcal{B}}_0$ and $\gamma_n = 2\pi\cdot 2.916$ rad.s^{-1}.G^{-1} is the neutron gyromagnetic ratio. Aligning the field boundaries parallel to the lattice planes, *i.e.* setting $\zeta = \pi/2 - \theta_B$ (*NLD condition*), cancels the velocity dependence of the phase (Eq. 3) and we find that this quantity is simply proportionnal to d on the one hand, and to user-defined quantities such as ω_L and L on the other hand. Then, it follows that any change in d will affect φ_{tot} accordingly:

$$\Delta\varphi_{tot} = \varphi_{tot}(d) - \varphi_{tot}(d_0) = \varphi_{tot}(d_0)\cdot\frac{\Delta d}{d_0} \tag{4}$$

where d_0 is to be taken as a reference. The latter equality obviously implies that relative evolution of the total phase is identical to the relative evolution of lattice constants under pressure, stress or temperature variation. Thus, the measurement of the relative evolution of d is done by slightly changing the field integral $\omega_L L$ and the intensity is modulated because the beam is finally analyzed. Another implication of Eq. 4 is that NLD allows to measure the lattice parameters distribution function width which can be retrieved by measuring the final polarization $\mathcal{P}_f$ of the beam as a function of total phase. Using Eq. 4, the latter quantity turns out to be the cosine Fourier transform of the lattice spacing distribution which is generally assumed to have a gaussian shape:

$$\mathcal{P}_f(\varphi_{tot},\delta) = \mathcal{P}_0\langle\cos\Delta\varphi_{tot}\rangle = \mathcal{P}_0\langle\cos\left[\varphi_{tot}\left(d_0\right)\cdot\frac{\Delta d}{d_0}\right]\rangle = \mathcal{P}_0\sum_i \exp\left(-\frac{\delta_i^2\varphi_{tot}^2\left(d_0\right)}{16\ln 2}\right) \qquad (5)$$

where $\mathcal{P}_0$ is the natural beam polarization, δ_i is the full width at half maximum of the individual lattice spacings distribution functions while i has to be equal to 1 for a true single crystal. Thus, in theory, increasing φ_{tot} provides a better resolution but also leads to a substantial depolarization of the beam and, in the extreme cases, it becomes more and more difficult to maintain high accuracy. We shall come back to this point later on.

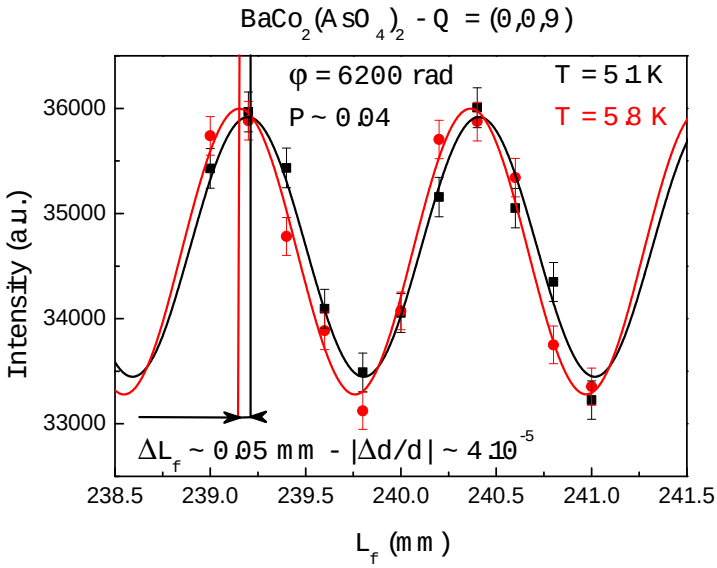

Figure 4. Typical signal measured with Neutron Larmor Diffraction. When d changes as a consequence of a temperature change, the signal is slightly shifted and the phase is recorded as the position of a local maximum. This example shows that a positionning accuracy of the translation stage of the order of 10 μm is needed to achieve a resolution $\Delta d/d \sim 10^{-5}$ at $\varphi_{tot} \sim 6200$ rad.

On the technical point of view, field regions are simulated by pairs of radio-frequency spin flippers (RFSFs). A RFSF consists of a flat solenoid which produces a homogeneous vertical static field $\vec{\mathcal{B}_0}$ and encloses radio-frequency coils producing a small oscillating field with frequency ω_{rf} and amplitude $\vec{\mathcal{B}_{rf}}$ in the horizontal scattering plane. When the RFSFs are set to resonance, *i.e.* when $|\vec{\mathcal{B}_0}| = \omega_{rf}/\gamma_n$, one pair simulates a field of magnitude $\mathcal{B}_0$ over a length

L, where L is the distance between coils ([6]). ZETA option is composed of 4 pairs of RFSFs which are located inside a double μ-metal shielding to avoid spurious magnectic fields which would induce unwanted beam depolarization (Fig. 3 *b)*). L can reach 172 cm in each arm (using the *Bootstrap* technique, [7]) and ω_{rf} can be varied up to 700 kHz which leads to a maximum Larmor phase of $\varphi_{tot}^{max} \sim 9 \cdot 10^3$ rad for the most commonly used wevelength, namely $\lambda = 2.36$ Å. This high limit is imposed in practice by the maximum current which can pass through the static coils wires which are water and air cooled and can produce at best a magnetic field of 240 G. Furthermore, using those flippers allows to modify the shape of the precession area as they can be easily rotated by an angle ζ with respect to the beam axis. In the case of ZETA, ζ can reach 70° which means that the *NLD condition* can be met in many cases.

With such a setup, the phase is measured by slightly changing the distances between coils in one of the two spectrometer arms[1]. The signal is modulated because this slight change in the field integral results in a small rotation of the final polarization. As the beam is analyzed by reflexion on a Heusler monochromator, the beam intensity can be fitted to a cosine law of the form $I_0\left(1+\mathcal{P}_f \cdot \cos\left(2\pi\frac{L-L_0}{w}\right)\right)$ where I_0 is the average intensity of the scattered beam, $\mathcal{P}_f$ its final polarization, w is the period of the signal and L_0 a reference length. Then, when d changes, the figure will be slightly shifted (for instance, see Fig. 4). To refine the phase change properly, one needs to record at least one period of the signal and to work with a sufficiently polarized beam. So things are simple if we refer to the formalism but we see that some difficulties may arise *e.g.* in the case of poor quality single crystals. There are in addition many sources of systematic errors which can not be avoided like thermal dilatation of the pieces composing the spectrometer or positionning errors of the translation stage. Those effect are on the other hand very small. Anyway, NLD potentially offers an appreciable gain in resolution in neutron diffraction whithout working with tight collimations, as it would be needed in CND, thanks to the aforementionned *NLD condition*.

4. Thermal expansion and magnetoelastic effect in $BaM_2(XO_4)_2$

Thermal evolution of the lattice parameters a (in-plane) and c (out-of-plane) in $BaM_2(XO_4)_2$ have been measured in each compounds using NLD. We used a neutron wavelength $\lambda = 2.36$ Å and worked with natural collimations $30' - 40' - 40' - 110'$[2]. The high temperature parts of each dilatation curves have been fitted to a simple polynomial model and extrapolated to T = 0. On the next step, this is considered as a "background" which is not linked with the magnetic ordering and is substracted from the raw curves. This is a mean to extract the "excess" lattice strain due to the magnetic ordering only.

4.1. $BaNi_2(PO_4)_2$

Thermal evolutions of a and c parameters have been inferred from the (2,0,2)[3] and (0,0,9) Bragg peaks respectively in a temperature range going from T = 1.5 up to 200 K. For both reflections, we worked at $\varphi_{tot} \simeq 6200$ rad which corresponds to a theoritical resolution of $\Delta d/d \simeq 8 \times 10^{-6}$. At the magnetic transition, a and c lattice parameters experience a strain which is respectively negative and positive (Fig. 5 a). The volumic magnetoelastic effect is

[1] This is possible because the last RFSFs pair is mounted on a translation stage.

[2] Collimations are given here in the usual order *i.e.* before monochromator, sample, analyzer and detector.

[3] In $BaM_2(XO_4)_2$ compounds, we have $c \gg a$ thus reflexions of the form (h,0,l) with h = 2 and $l = \overline{1}, 2$ mainly reflect a^*. In the case of $BaNi_2(PO_4)_2$ and $BaNi_2(AsO_4)_2$, the angle betwen $\vec{Q} = (2,0,2)$ and $\vec{a^*}$ is $\sim 10°$ while in $BaCo_2(AsO_4)_2$ we get, between $\vec{Q} = (2,0,\overline{1})$ and $\vec{a^*}$, an even smaller angle of $\simeq 5°$.

obtained through $\Delta V/V = 2\Delta a/a + \Delta c/c$[4] and is slightly negative *i.e.* the unit cell undergo a weak spontaneous contraction at T_N (Fig. 5 c). At T = 0, we find $\Delta V/V \sim -4 \cdot 10^{-5}$. On Fig. 5 *b)* and *c)*, we report the relative lattice parameters and volume variations as a function of the intensity of the (2,0,2) Bragg peak, itself proportional to the square of the magnetic moment. We note that this peak is both structural and magnetic. This implies that it may be subjected to extinction at the transtion but this effect is in this case negligible because the nuclear structure factor is weak. Direct scaling to the square of the magnetic moment (Fig. 2) indeed gives a similar result. Correlation between both quantities is quite good which indicates that the unit cell volume is a quadratic function of the order parameter. This result is expected for single lattice ferromagnets but has also been observed in the two sublattices antiferromagnets transition metals difluorides MF_2 ([8]). This spontaneous strain is very weak in magnitude but can be resolved thanks to the high accuracy provided by NLD.

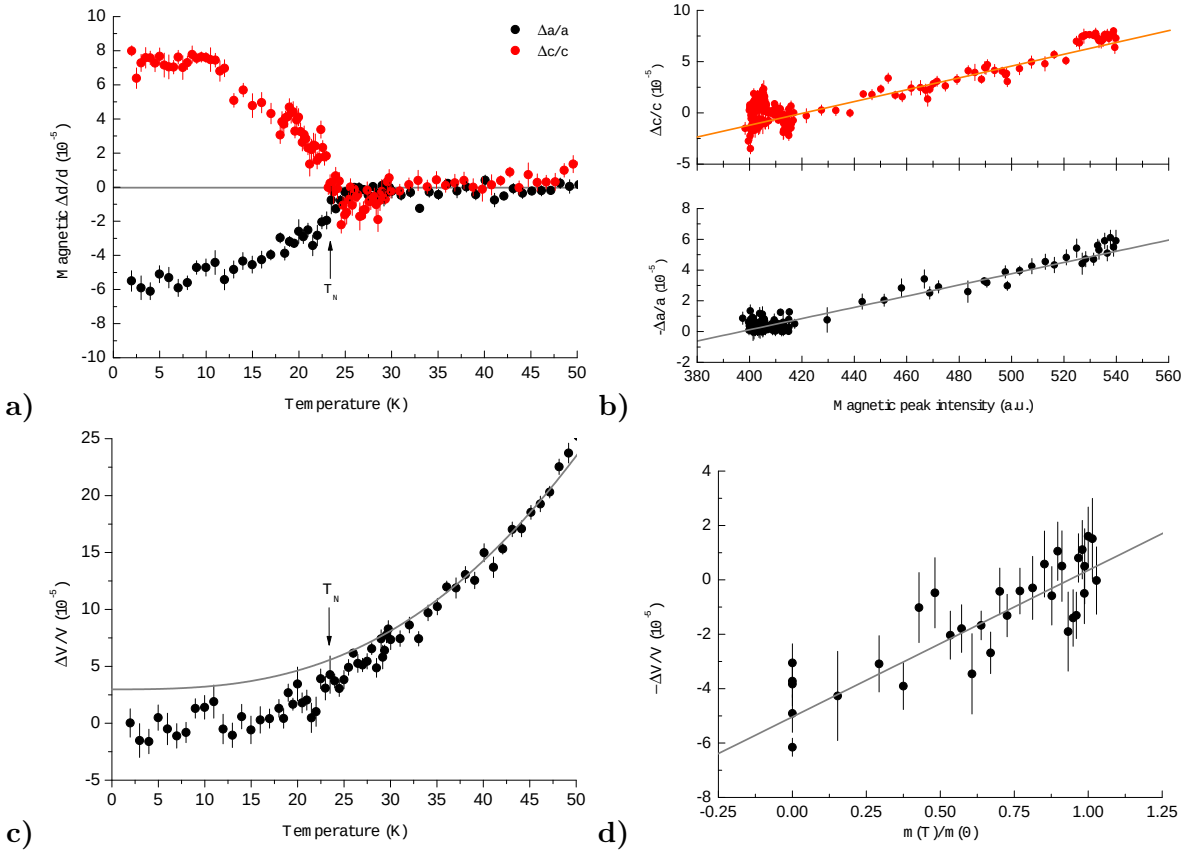

Figure 5. Magnetoelastic effect in $BaNi_2(PO_4)_2$. *a)* Thermal variation of the "excess" axial strain induced in the ordered phase. *b)* Axial strains as a function of (2,0,2) magnetic peak intensity (see text). *c)* Relative variation of the unit cell volume. Solide line is the sum of polynomial fits performed on the high temperature axial expansion data (see text). *d)* Volumic strain as a function of the ordered magnetic moment.

[4] Volume dilatation coefficient β is equal to the trace of the linear thermal dilatation tensor. In the case of hexagonal unit cell, we simply get $\beta = \frac{dV}{VdT} = 2\frac{da}{adT} + \frac{dc}{cdT}$ which leads to the above relation.

4.2. $BaCo_2(AsO_4)_2$ and $BaNi_2(AsO_4)_2$

The situation is rather different in baryum arsenides. For instance, in $BaCo_2(AsO_4)_2$, the magnetic strain goes in opposite sense as compared with the previous case, being respectively positive and negative for a and c lattice constants. The measurement has been made at $\varphi_{tot} = 4300$ and 6200 rad for the $(2,0,\bar{1})$ and (0,0,9) respectively between 2 and 60 K. Expected resolution is therefore of the order of 8×10^{-6} and 1×10^{-5} which is enough to resolve the very steep lattice constant variation along both directions (Fig. 6 a). The volumic effect at T = 0 is positive with $\Delta V/V \simeq +10^{-4}$. The situation is then clearly different as compared with the observations made in $BaNi_2(PO_4)_2$ even though the steeper moment variation gives a steeper lattice constant evolution at the magnetic transition.

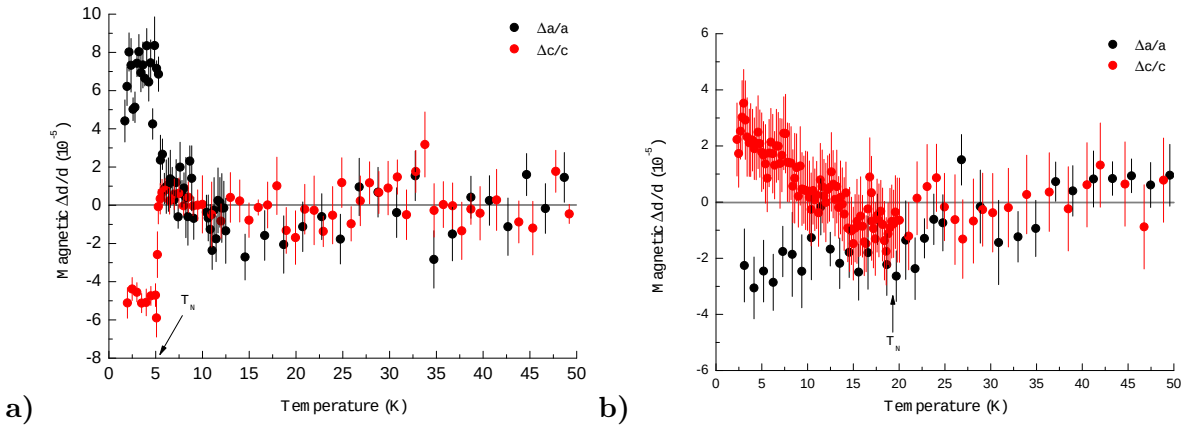

Figure 6. *a)* Axial magnetoelastic effect in $BaCo_2(AsO_4)_2$. The magnetic transition is marked by a step-like variation in lattice constants. *b)* Axial magnetoelastic effect in $BaNi_2(AsO_4)_2$. In this case, it is barely resolved but still visible (see text).

The experiment with $BaNi_2(AsO_4)_2$ has been more difficult to conduct as the polarization decay was is in this case rather fast when increasing φ_{tot} (a consequence of the large lattice spacing distribution, from Eq. 5.). For this measurement, we could only achieve a modest resolution of about 10^{-4} and 1.7×10^{-5} for the (2,0,2) and (0,0,9) reflection respectively. This is not good engouh to clearly resolve the volumic magnetoelastic effect but it nevertheless seen. From the data, we obtain an estimation of $\Delta V/V \simeq -3 \times 10^{-5}$ (Fig. 6 b).

5. Conclusion and outlook

We have investigated magnetoelastic properties of $BaM_2(XO_4)_2$ compounds using Neutron Larmor Diffraction. Our results show that in the case of $BaNi_2(PO_4)_2$ and $BaCo_2(AsO_4)_2$, magnetostriction is strongly correlated to the square of the order parameter, namely the value of the ordered magnetic moment. Strains are found to be weak but we were able to resolve them thanks to the high resolution provided by NLD. For the first sample, there is a volume contraction at T_N while the second one experience an expansion. The case of $BaNi_2(AsO_4)_2$ is more difficult because the relatively large lattice spacing distribution led to a substantial depolarization of the beam. Consequently, the measurement has been conducted at a rather poor resolution and the magnetoelastic effect is only barely resolved but seems to exist anyway. A rough estimation gives a negative value for the relative volume variation. In those three cases, we indeed observe an isostrucural transition at T_N. The way the lattice responds to magnetic ordering depends in

a non-trivial way on the value of the spin or the magnetic structure propagation vector. Now, the next step in the understanding of the magnetostructural phase transitions in $BaM_2(XO_4)_2$ would require theoritical work to be done to link our thermal expansion result with a physical model. We hope that those results will trigger new studies aiming to understand the magnetic and structural behaviours in this interesting family with 2-d topology and honeycomb magnetic network.

Acknowledgments

We would like to aknowledge technical support by B. Geffray, B. Longuet and F. Mantegazza during the course of the experiments. This work has been supported by the FRENCH ANR project NEMSICOM and the European NMI3 network under Contract HII3-CT-2003-505925.

References

[1] Lee S., Pirogov A., Kang M., Kwang-Hyun J., Yonemura M., Kamiyama T., Cheong S.-W., Gozzo F., Namsoo S., Kimura H., Noda Y. and Park J.-G. 2008 *Nature* **451** 805-8
[2] Martin N., Regnault L.-P., Klimko S., Lorenzo J.E. and Gaehler R. 2011 *Physica B: Condensed Matter* **406** 2333-36
[3] Regnault L.-P. and Rossat-Mignod J. 1990 *Magnetic Properties of Layered Transition Metal Compounds* ed De Jongh L.J. (Kluwer Academic Press) 271-321
[4] Regnault L.-P. 1981 *PhD thesis*
[5] Rekveldt M.T.H. and Kraan W.H 1999 *J. Neutron Research* **8** 53-70
[6] Golub R. and Gaehler R. 1987 *Phys. Lett. A* **123** 43-48
[7] Gaehler R. and Golub R. 1988 *J. Phys. France* **49** 1195-1202
[8] Chatterji T., Iles G.N., Ouladdiaf B. and Hansen T.C. 2010 *J. Phys. Condens. Matter* **22** 316001